N 69 26439

NASA CR 101115

THE UNIVERSITY OF MICHIGAN
ANN ARBOR, MICHIGAN

SEMIANNUAL PROGRESS REPORT NO. 5

ON

MICROWAVE DEVICE INVESTIGATIONS

This report covers the period October 1, 1968 to April 1, 1969

Electron Physics Laboratory
Department of Electrical Engineering

By: W. R. Curtice
W. D. Getty
G. I. Haddad
R. J. Lomax

Approved by: G. I. Haddad
G. I. Haddad, Director
Electron Physics Laboratory

Project 08400

RESEARCH GRANT NO. NGL 23-005-183
OFFICE OF SPACE SCIENCE AND APPLICATIONS
NATIONAL AERONAUTICS AND SPACE ADMINISTRATION
WASHINGTON, D. C. 20546

April, 1969

TABLE OF CONTENTS

LIST OF ILLUSTRATIONS

PUBLICATIONS DURING THE LAST PERIOD

Konrad, G. T., "Harmonic Generation in Nonlinear Beam-Plasma Systems," Tech. Report No. 112, Contract No. NGL 23-005-183, Electron Physics Laboratory, Department of Electrical Engineering, The University of Michigan, Ann Arbor; January, 1969.

Krumm, C. F. and Haddad, G. I., "Millimeter- and Submillimeter-Wave Detection by Paramagnetic Materials," To be presented at the 1969 IEEE G-MTT International Microwave Symposium, Dallas, Texas; May, 1969.

Konrad, G. T., "Ion Implantation in Semiconductors," EPL Memo No. 69-2-08400, Electron Physics Laboratory, Department of Electrical Engineering, The University of Michigan, Ann Arbor; January 17, 1969.

SEMIANNUAL PROGRESS REPORT NO. 5

ON

MICROWAVE DEVICE INVESTIGATIONS

1. General Introduction (G. I. Haddad)

This report covers the work performed during the period October 1, 1968 to April 1, 1969. A brief description of the work performed during this period as well as the plans for the coming period are described below.

The tasks which were continued from the previous period and their status are as follows:

a. Beam-Plasma Interaction for Amplification and Harmonic Generation. The work under this phase of the program consisted of two parts. The first was concerned with amplification, harmonic generation and coupling schemes in a beam-plasma system. It was performed by G. T. Konrad and J. E. Rowe. This work has been completed and a technical report describing it has been issued. Mr. Konrad did this work for his Ph.D. dissertation and he is presently at M.I.T. Lincoln Laboratory. An abstract of his dissertation follows:

"The purpose of this study is to investigate both theoretically and experimentally the saturation characteristics of beam-plasma devices. The gain, power output, efficiency and the magnitude of the higher harmonic components that pertain to such devices are of particular interest.

The geometry treated in this study consists of a cylindrical plasma column which serves as a slow-wave circuit along which electromagnetic energy can propagate. A cylindrical electron stream is assumed to be concentric with the plasma column. Amplification of an RF signal takes place when a fraction of the kinetic energy of the stream electrons is converted into RF wave energy.

The plasma is assumed to remain linear during the interaction process so that it is possible to derive an equivalent circuit for which the various elements are given in terms of the plasma parameters. Beam and plasma collisions are included in the analysis and give rise to lossy elements in the equivalent circuit. The electron stream is shown to become nonlinear much more easily than the plasma so that it is justifiable to treat only the stream in a nonlinear fashion. A Lagrangian (ballistic) analysis is used to calculate the trajectories of the various charge groups into which the electron stream is subdivided. One- as well as two-dimensional stream models are used. A digital computer is employed to calculate both the charge group trajectories and the RF currents and circuit voltages of the fundamental signal and its harmonics generated by the nonlinear operation. Intermodulation and cross-modulation effects in multisignal operation are also studied.

An experimental test vehicle is described which permits correlation of the theoretically calculated results with those obtainable from an actual beam-plasma interaction. A xenon plasma column 10.5 cm long is generated by either a hot cathode Penning discharge or by ionization due to the beam electrons passing through the xenon gas. Values of electronic gain as high as 35 dB in the vicinity of 2.0 GHz are obtained experimentally by the latter scheme. Harmonic components through the fifth are observed with the second harmonic being only 5 dB below the fundamental under certain conditions. When collision effects are taken into account in the theoretical calculations, it is shown that the agreement with the experimentally observed values is quite good for the cases that can be compared.

Coupling of RF energy into and out of the beam-plasma device is considered in detail theoretically and experimentally. Short sections of

a slow-wave structure outside of the plasma region are used in the device under test for much of the experimental work. Another coupling scheme making use of quasi-optical techniques is a set of elliptic cavity couplers. These are found to yield a coupling loss of only 10 to 15 dB per coupler over a frequency range of slightly greater than 20 percent in the low S-band frequency region. This coupling approach is much less lossy than most other methods employed previously. Efforts to use these couplers for RF amplification measurements are shown to be unsuccessful due to cathode poisoning at the higher gas pressures required."

The second part is concerned with a theoretical evaluation of the dispersion relations for beam-plasma interaction under more realistic situations. This work is being performed by J. D. Gillanders and R. J. Lomax. Mr. Gillanders is doing this work for his Ph.D. dissertation. This work has been completed and a technical report describing it is presently being prepared. It should be completed in the near future.

b. Electron-Beam Cyclotron-Harmonic Instabilities: The corkscrew magnetic field arrangement for producing transverse velocities in an electron beam has been evaluated further and some results are reported. A study of instabilities will be performed during the coming period.

c. Millimeter- and Submillimeter-Wave Detectors: The paramagnetic downconverter has been evaluated at liquid nitrogen temperature and a noise equivalent power of approximately -90 dBm has been achieved so far. Schemes for improving this and an evaluation of the detector at liquid helium temperature will be performed during the coming period.

The work on bulk semiconductor materials for use at millimeter wavelengths was continued during this period. A theoretical field formulation for a semiconductor sample in a cavity was performed. This is essential for

the measurement of semiconductor properties. The theoretical and experimental work on the utilization of bulk semiconductor materials for millimeter-wave detection and harmonic generation will be continued during the coming period.

The new tasks which were initiated during this period include the following:

1. Millimeter-Wave Gunn-Effect Devices: This phase of the program is presently concerned with a theoretical formulation of the LSA mode. It is planned to include various mechanisms which are present in the material but have not been taken into consideration previously. Some of these mechanisms become very important at higher frequencies.

2. Two-Dimensional Analysis of Avalanche-Diode Oscillators: The purpose of this phase of the program is to obtain a two-dimensional analysis of an avalanche-diode oscillator. It is hoped this will contribute to the understanding of such devices and to explain some of the properties which have not been explained from the one-dimensional analyses which have been performed.

3. Ion Implantation in Semiconductors: Some preliminary work was performed during this period concerning the possibility of converting the equipment which was employed in the Cerenkov radiation experiment into an ion implantation machine. A summary of this work is presented in an attached memorandum by G. T. Konrad. The University has provided the necessary funds for this purpose and work on this will be initiated shortly.

2. Beam-Plasma Interactions

Supervisor: R. J. Lomax

Staff: J. D. Gillanders

2.1 Introduction. The presence of gain or of an instability in a beam-plasma interaction can be determined by examining the dispersion

equation of the interaction. Simplified theories which ignore collisions, finite temperature effects and some or all of the boundary conditions predict gain and instabilities much stronger than are observed experimentally. In the simplest cases infinite gains are predicted. However, when the above factors are not ignored, the dispersion relation becomes much more complicated. Therefore, a very efficient method is needed to solve the equation if information about the interactions is to be obtained in a reasonable amount of computation time. A new approach to this problem has been outlined in previous reports. Results are currently becoming available from this method.

2.2 Conclusions. Since the last report the Calcomp plotting program has been written and checked out. From the results plotted so far it appears that the model is giving fairly good agreement with experimentally observed results.

The effect of finite temperature broadens the band over which gain is found, as expected, but decreases the magnitude of the gain available. The collisions reduce the magnitude of the gain but have little effect on the bandwidth.

2.3 Program for the Next Period. A final report on this portion of the work is now being prepared. It is expected that this final report will be ready for publication in the near future.

3. The Study of Cyclotron Harmonic Instabilities

Supervisor: W. D. Getty

Staff: A. Singh

This part of the project is devoted to the study of cyclotron harmonic instabilities in plasmas with anisotropic velocity distributions.

The device proposed for creating the required velocity distribution is the Wingerson-type corkscrew. The axial-to-transverse velocity conversion

characteristics of the corkscrew are being studied on an electron-beam velocity analyzer. The corkscrew is designed to give an axial-to-transverse velocity conversion ratio of 0.4 at a beam voltage of 576 V and at a magnetic field of 190 G. It was reported in the last semiannual progress report that the corkscrew operates satisfactorily at other beam voltages and axial magnetic field strengths provided $\sqrt{V_o}/B_o$ is kept constant. Figures 3.1 show some of the results obtained with beam voltages of 200 V, 400 V and 576 V for various values of corkscrew currents. It will be appropriate here to describe the velocity analyzer briefly before explaining the curves shown in Figs. 3.1.

The axial velocity analyzer consists of a beam current collector with a pinhole of 0.010 inch diameter through which a small part of the beam is sampled. Behind this aperture is a gridded cylinder (retarding electrode) whose potential can be varied from that of the gun cathode to that of the anode. At the other end of this cylinder is an analyzer collector held at the same potential as the beam collector (system ground potential). The gridded cylinder acts as the retarding electrode. When the axial energy of the beam is less than the potential difference between the beam collector and the retarding electrode, no current will be observed at the analyzer collector. It may be shown that the retarding electrode potential at which the current begins to flow is a measure of the transverse energy of the beam. It may be noted that all voltages are measured with respect to the cathode. Thus

$$\text{conversion ratio} = \frac{v_\perp}{v_o} = \left[\frac{\text{retarding electrode potential at cutoff}}{\text{beam voltage } V_o}\right]^{1/2}$$

In Figs. 3.1 the analyzer collector current is plotted against retarding electrode potential. For purposes of calculation, the cutoff

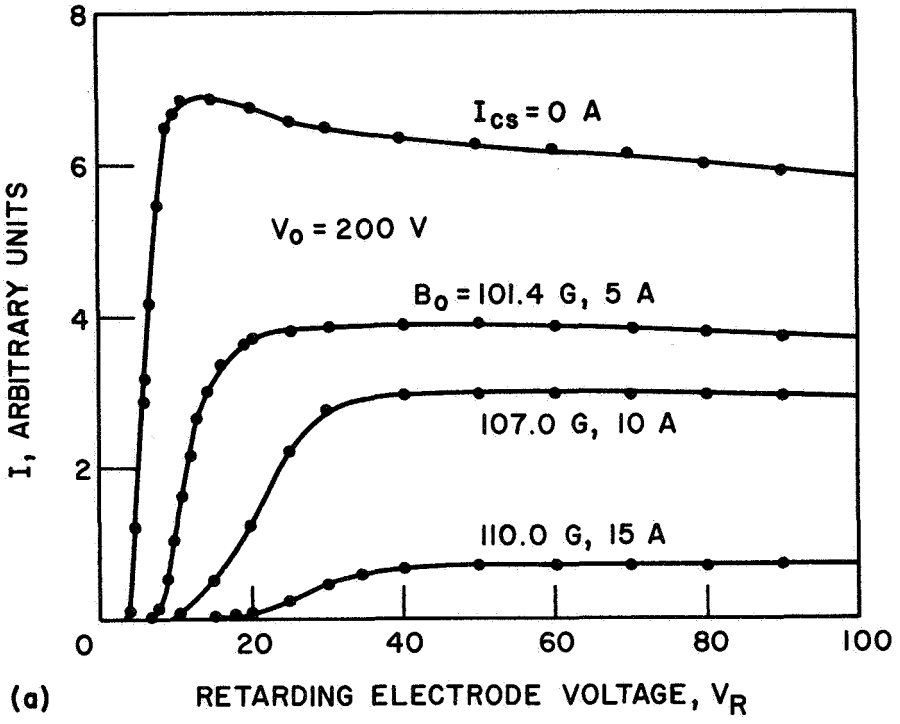

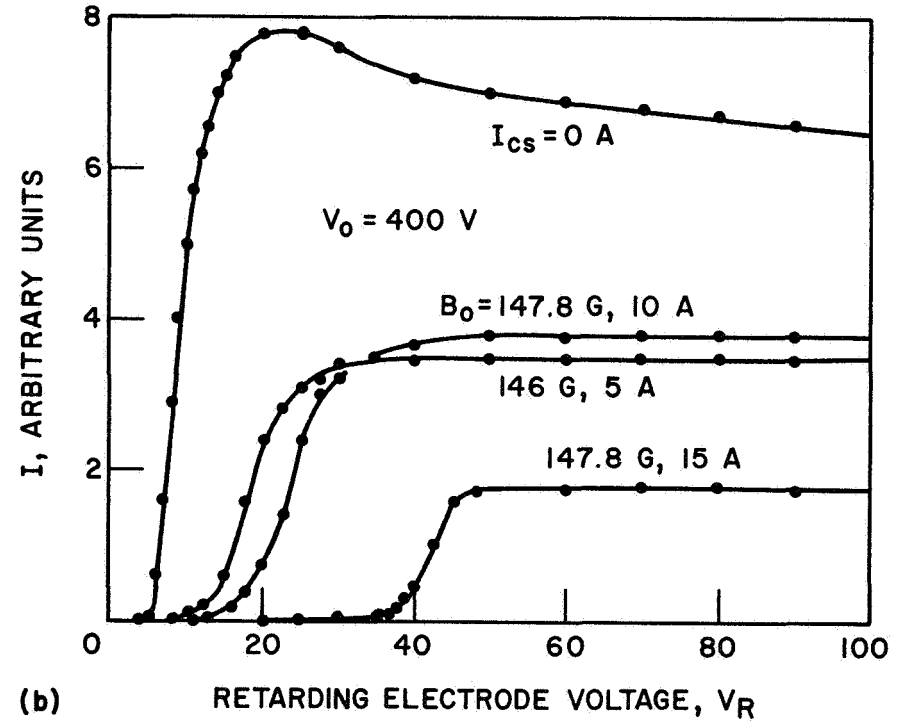

FIG. 3.1a,b VELOCITY ANALYZER COLLECTOR CURRENT (ARBITRARY UNITS) VS. RETARDING ELECTRODE POTENTIAL WITH AXIAL MAGNETIC FIELD AND CORKSCREW CURRENT AS PARAMETERS. (a) BEAM VOLTAGE V_o = 200 V AND (b) V_o = 400 V.

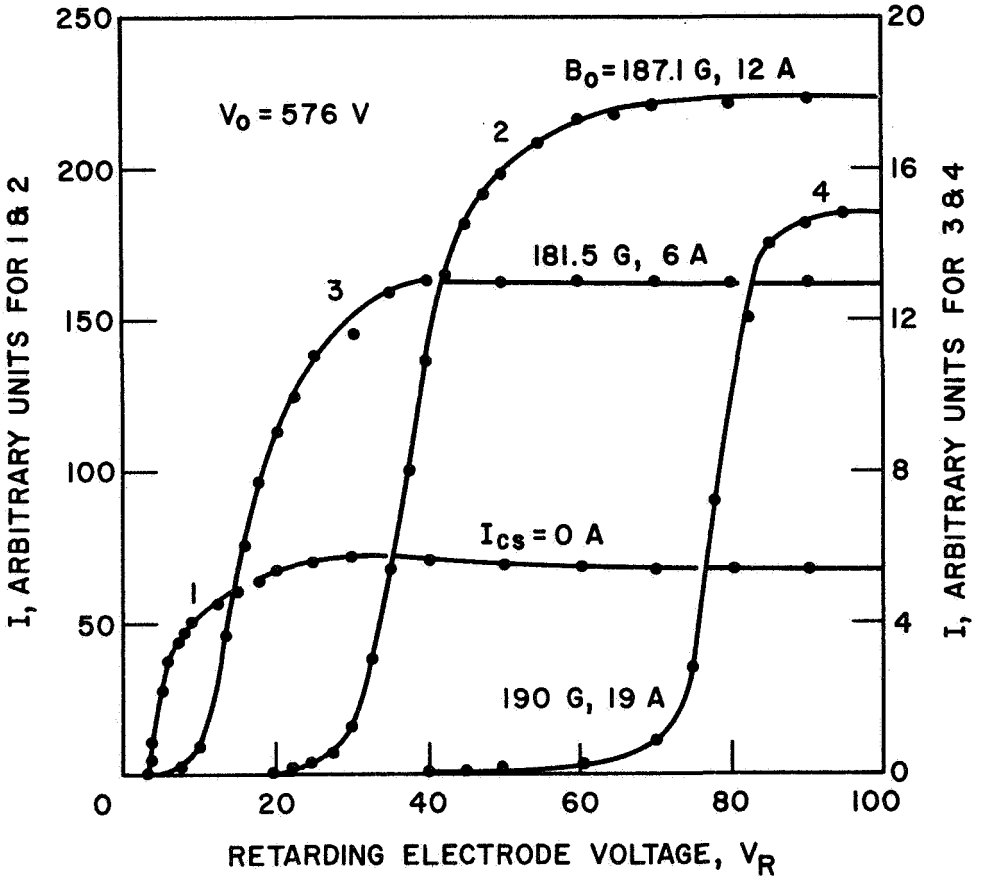

FIG. 3.1c VELOCITY ANALYZER COLLECTOR CURRENT (ARBITRARY UNITS) VS. RETARDING ELECTRODE POTENTIAL WITH AXIAL MAGNETIC FIELD AND CORKSCREW CURRENT AS PARAMETERS. BEAM VOLTAGE V_o = 576 V.

potential is taken as that potential where the analyzer collector current reaches one-tenth of its saturation value.

As indicated on each curve, the axial magnetic field varies slightly from curve to curve. Slight tuning in axial magnetic field strength is required to obtain sharp cutoff and straight and parallel curves. The effect of slight variations in B_o on the axial velocity distribution of the beam at the output of the corkscrew is shown in Fig. 3.2. It can be seen from these curves that, unless B_o is adjusted properly, the velocity distribution at the output of the corkscrew can vary considerably. The maximum change in B_o in Fig. 3.2 is only 7.1 percent. From these curves it can also be seen that diamagnetic measurements on such a beam will not give proper information about the transverse velocity distribution.

From the same data used for the curves shown in Figs. 3.1, we can calculate the velocity conversion ratio for V_o = 200 V, 400 V and 576 V for the corkscrew currents indicated on the figure. In Fig. 3.3 this ratio is plotted against corkscrew currents. The solid lines in Fig. 3.3 are drawn from computer results for corkscrews designed keeping

$$\frac{\sqrt{V_o}}{B_o} = \frac{\sqrt{576}}{190} \ \frac{\text{volts}^{1/2}}{\text{gauss}} \ .$$

The data at this stage is rather meager to warrant any general conclusions. However the distribution of points about their respective computer curves is fairly even.

3.1 Program for the Next Period. At the time of writing this report, the tube is operating and further measurements are being carried out.

The experimental setup, for measurement of propagation characteristics of microwaves on beams with anisotropic velocity distribution and detection of associated instabilities, has been designed and is presently being fabricated.

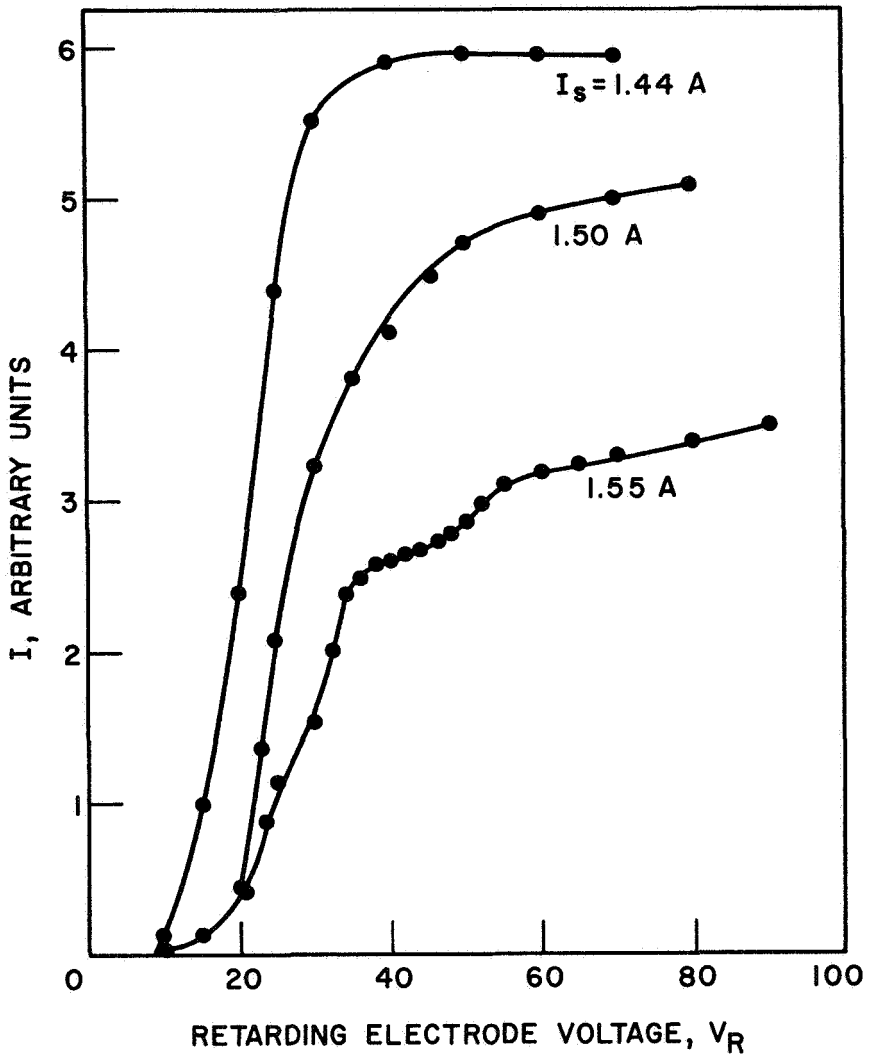

FIG. 3.2 ANALYZER COLLECTOR CURRENT VS. RETARDING ELECTRODE POTENTIAL SHOWING THE EFFECT OF VARIATION OF B_o ON THE VELOCITY SPREAD IN THE ELECTRON BEAM AT THE OUTPUT OF THE CORKSCREW. FOR ALL CURVES, V_o = 200 V AND I_{cs} = 10 A.

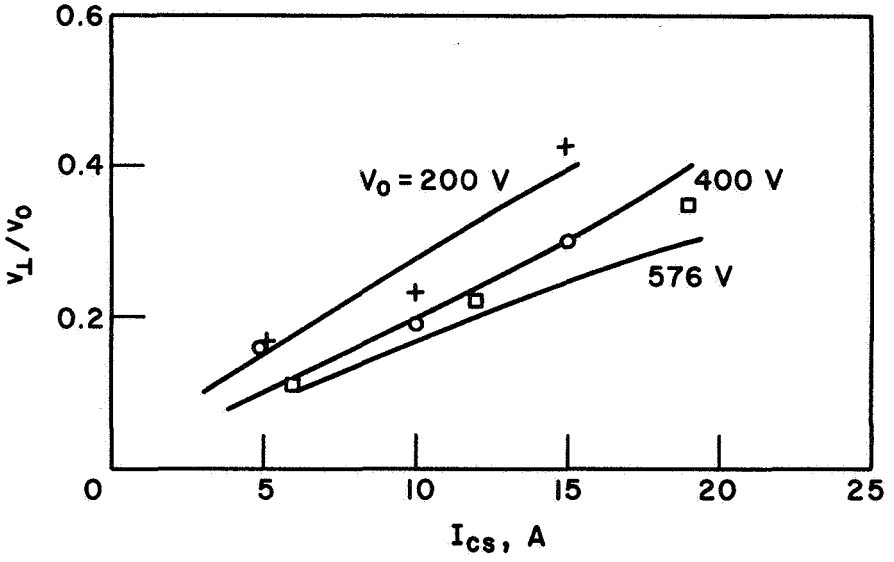

FIG. 3.3 WINDUP RATIO $v_\perp/v_o$ VS. CORKSCREW CURRENT. (SOLID LINES GIVE THE RELATIONSHIP BETWEEN THE TWO QUANTITIES IF THE CORKSCREW WERE DESIGNED WITH $\sqrt{V_o}/B_o = 1263$ MKS AND WITH THE BEAM VOLTAGES SPECIFIED IN FIG. 3.3. + , o AND □ ARE EXPERIMENTAL POINTS FOR 200 V, 400 V AND 576 V AS THE BEAM VOLTAGES, RESPECTIVELY. B_o AT EACH POINT WAS ADJUSTED TO GET MINIMUM SPREAD IN AXIAL ENERGY.)

4. Paramagnetic Materials for Millimeter- and Submillimeter-Wave Detection

Supervisor: G. I. Haddad

Staff: C. F. Krumm

The purpose of this phase of the program is to investigate the feasibility of using paramagnetic materials to detect millimeter- and submillimeter-wave radiation. The downconversion scheme currently being studied is similar in principle to a three-level maser. Two signals, one a millimeter-wave frequency and the other a microwave frequency, are partially absorbed by a paramagnetic material. The power reflected at the microwave frequency depends upon the power incident at the millimeter-wave frequency. Monitoring the changes in reflected microwave power corresponds to detection of the millimeter-wave signal.

Extensive experimental tests have been run on the paramagnetic downconverter at liquid nitrogen temperatures. The change in microwave output due to the millimeter-wave input can be characterized by the formula

$$\Delta P_r = \frac{(P_{mm} P_i)/P_c}{1 + P_i/P_{sat}} , \qquad (4.1)$$

where ΔP_r = the change in microwave reflected power,

P_i = the incident microwave power,

P_{mm} = the incident millimeter-wave power,

P_c = a constant and

P_{sat} = the saturation input power at the microwave frequency.

Typical numbers for liquid nitrogen temperatures are $P_c = 1.5$ W, and $P_i = P_{sat} = 1.5$ mW. These give an overall conversion loss of 33 dB

The overall conversion loss includes both the internal conversion loss of the device and the mismatch losses at the input and output frequencies. The millimeter-wave input mismatch loss is defined as the

ratio of the power absorbed by the spin system to the incident power. This can be expressed mathematically as

$$L_{input} = 2(\rho_m - \rho_o)\left(\frac{1 - \rho_m}{1 - \rho_o}\right) , \qquad (4.2)$$

where ρ_m = the cavity reflection coefficient with magnetic resonance and

ρ_o = the cavity reflection coefficient with no magnetic resonance.

In a similar way, the output mismatch loss is defined as the ratio of the observed change in reflected power to the change in power absorbed by the spin system. This can be written as

$$L_{output} = \frac{\rho_m(1 - \rho_o)}{1 + \rho_o - 2\rho_m} . \qquad (4.3)$$

At liquid nitrogen temperatures these losses are approximately 17 dB. Using the figures given above, the minimum attainable conversion loss is 30 dB. This implies that the internal conversion loss is 13 dB. For the operating points discussed here, the minimum possible conversion loss with equal relaxation rates between all levels is 9 dB.

Attempts to measure the response time at liquid nitrogen temperatures have been only partially successful. The relaxation time of the microwave levels has been measured using CW saturation methods.[1] These times are on the order of 10 μs. Attempts to measure the device response time by pulsing the millimeter-wave source and examining the microwave response have not been successful. This is due mainly to a limitation in the millimeter-wave klystron power supply.

---

1. Eschenfelder, A. H. and Weidner, R. T., "Saturation Effects on Paramagnetic Resonance," Phys. Rev., vol. 92, No. 4, pp. 869-873; November 15, 1953.

Some preliminary measurements of the noise of this device have been obtained. These indicate that the noise contributed by the device itself is negligible in comparison with that of the following amplifier. This is as expected since the device noise temperature is usually less than twice the bath temperature and this is well below the equivalent temperature of the following amplifiers.

The minimum detectable power for this system can be determined approximately from the equation

$$(P_{mm})_{min} = \frac{V_n P_c}{RP_i} , \qquad (4.4)$$

where R = the responsivity of the output detector and

V_n = the noise voltage due to the amplifiers following the downconverter.

For $P_c = 1$ W, $RP_i = 1$ V and $V_n = 1$ μV, $(P_{mm})_{min} = 1$ μW. This is near the measured liquid nitrogen temperature results obtained with a circulator.

These results can be significantly enhanced through the use of a magic T or similar bridge setup. Unfortunately the current experiment is not well suited to this purpose. The paramagnetic material has poor thermal contact with the bath and temperature fluctuations tend to make the balance drift rapidly.

Some additional liquid nitrogen temperature measurements will be made in the next period. Also some of the liquid helium measurements will be repeated using refined measurement techniques.

5. Bulk Semiconductor Materials for Millimeter- and Submillimeter-Wave Detection

Supervisor: G. I. Haddad

Staff: I. I. Eldumiati

The objective of this phase of the program is to study suitable bulk semiconductor materials for applications in the millimeter- and submillimeter-wave region. In order to study the material interaction with electric and magnetic fields, cavity perturbation techniques using both equivalent circuit and field theory approaches are under investigation.

The equivalent circuit of the bulk material in a reflection-type reentrant cavity has been developed. The introduction of the material in the cavity produces a change in the resonant frequency and the power reflected from the cavity. The conductivity and dielectric constant of the material are expressed in terms of the change in the reflected power, the frequency shift and other measurable quantities such as the Q-factor and the coupling coefficient of the cavity before and after the material is introduced. Optimization of the scheme is being studied as a function of the coupling factor and the material parameters. A computer program is being written for this purpose. A fixed-size cavity resonant at an X-band frequency was built, and the circuit explained in Semiannual Progress Report No. 3 was used to verify the theoretical and numerical results. The method will be extended to study the change in the material parameters with temperature and magnetic fields at other frequency bands.

It can be shown that

$$\frac{f_r - f_{ro}}{f_r} + \frac{1}{2Q_L}\left(\frac{1}{Q_L} - \frac{1}{Q_{Lo}}\right) + j\,\frac{1}{2}\left(\frac{1}{Q_L} - \frac{1}{Q_{Lo}}\right)$$

$$= \frac{\int_{V_s}[(\mu - \mu_o)\underline{H}\cdot\underline{H}_o - (\epsilon - \epsilon_o)\underline{E}\cdot\underline{E}_o]\,dV}{\int_{V_c}(\epsilon\underline{E}\cdot\underline{E}_o - \mu\underline{H}\cdot\underline{H}_o)\,dV}\,, \quad (5.1)$$

where f_r = the resonance frequency of the cavity,

Q_L = the loaded Q-factor of the cavity,

μ = the permeability of the medium,

ϵ = the permittivity of the medium,

V_s = the sample volume,

V_c = the volume of the cavity and

$\underline{E},\underline{H}$ = the electric and magnetic fields.

The subscript o denotes quantities in the absence of perturbation.

If the material is placed in the high electric field region under the central post of the cavity, with its sides parallel to the electric field lines, then the continuity of the tangential components of electric fields together with the orthogonality of electric and magnetic fields imply:

$$\underline{E} = \underline{E}_o$$

and

$$\mu_o\underline{H}_o = \mu\underline{H}$$

over the size of the sample. Hence Eq. 5.1 becomes:

$$\frac{f_r - f_{ro}}{f_r} + \frac{1}{2}\left(\frac{1}{Q_L^2} - \frac{1}{Q_L Q_{Lo}}\right) + \frac{j}{2}\left(\frac{1}{Q_L} - \frac{1}{Q_{Lo}}\right)$$

$$= \frac{\left(\mu_o - \frac{\mu_o^2}{\mu}\right)\int_{V_s}|H|^2\,dV - (\epsilon - \epsilon_o)\int_{V_s}|E|^2\,dV}{\int_{V_c}\left(\epsilon_o|\underline{E}|^2 + \frac{\mu_o^2}{\mu}|\underline{H}|^2\right)dV}\,. \quad (5.2)$$

If $\mu = \mu_o$, which is true in our case, then Eq. 5.2 reduces to:

$$\frac{f_r - f_{ro}}{f_r} + \frac{1}{2}\left(\frac{1}{Q_L^2} - \frac{1}{Q_L Q_{Lo}}\right) + \frac{j}{2}\left(\frac{1}{Q_L} - \frac{1}{Q_o}\right) = \frac{-\frac{1}{2}\left(\frac{\epsilon}{\epsilon_o} - 1\right)\int_{V_s} |\underline{E}|^2 \, dV}{\int_{V_c} |\underline{E}|^2 \, dV}$$

$$= \alpha\left(\frac{\epsilon}{\epsilon_o} - 1\right) , \quad (5.3)$$

where

$$\alpha = -\frac{1}{2} \frac{\int_{V_s} |\underline{E}|^2 \, dV}{\int_{V_c} |\underline{E}|^2 \, dV} .$$

Equation 5.3 shows that the material properties can be determined by measuring the cavity parameters before and after perturbation and knowing the field distribution within the cavity. The fields inside the cavity were expanded as a Fourier series, whose coefficients were determined by using the proper boundary conditions, together with cylindrical harmonic expansions. A computer program was developed, which solves for the Fourier coefficients as a function of the cavity dimensions. This takes care of determining the constant α in Eq. 5.3 to within a multiplying factor.

In the next period the cavity perturbation techniques will be continued. Theoretical investigation of the complex dielectric constant ϵ and its dependence on electric and magnetic fields will be studied.

Also, experimental work will be continued to verify the theoretical results. Experiments will be carried out at frequencies in the X-, Ku- and E-bands.

6. Millimeter-Wave Gunn-Effect Devices

Supervisor: W. R. Curtice

Staff: J. J. Purcell

6.1 Introduction. For a better understanding of the operation and limitations of LSA-mode, Gunn-effect devices at millimeter wavelengths, it is necessary to evaluate the effects of the following phenomena:

1. Intervalley transfer time.
2. Formation of accumulation layers.
3. Doping fluctuations.

Furthermore, the analysis should include transverse boundary conditions and, in particular, the skin effect.

6.2 Summary of Initial Studies. In the initial stages of this project, a simple two-valley conduction-band model has been used. The average carrier temperature is determined by the one-dimensional energy transport equation and the instantaneous energy distribution of carriers is related to the average temperature by a modified Maxwell-Boltzmann function. Carrier streaming is neglected and the rate of carrier energy relaxation toward an equilibrium distribution is assumed to be rapid compared with the reciprocal of the dielectric relaxation time.

Solutions of drift velocity as a function of time have been obtained for operation over a wide frequency range, and the analysis yields conductance, susceptance and efficiency values which are in general agreement with observed behavior and the results of other workers.[1,2]

---

1. Butcher, P. N. and Hearn, C. J., "Theoretical Efficiency of the LSA Mode for Gallium Arsenide at Frequencies Above 10 GHz," Electronics Letters, vol. 4, No. 21, pp. 459-461; October, 1968.

2. Ohmi, T. et al., "Effect of Intervalley Scattering Time on LSA Oscillations," Proc. IEEE, vol. 56, No. 4, pp. 747-748; April, 1968.

In Fig. 6.1, the dynamic solution at a frequency of 7 GHz shows how the relaxation time for intervalley scattering has an effect on LSA oscillation at frequencies that are low compared with the reciprocal relaxation time of 870 GHz. The static curve lies close to the experimental results of Ruch and Kino.[3] The static drift velocity corresponding to the bias field (10 kV/cm) is used as an initial approximation to the dynamic solution. Successive cycles then follow the dynamic solution exactly. The assumed RF field amplitude of 7.7 kV/cm results in 14.8 percent efficiency, which is only 0.1 percent less than that obtained using the static curve.

6.3 Program for the Next Period. In the next period, the effect of nonsinusoidal RF fields on efficiency will be investigated and, subsequently, the effect of accumulation layers will be included.

7. Two-Dimensional Analysis of Avalanche-Diode Oscillators

Supervisor: R. J. Lomax

Staff: M. S. Gupta

7.1 Introduction. A study of the effects of nonuniformities in the transverse cross section of avalanche diodes was initiated in this period. It is aimed at explaining several experimentally observed characteristics of avalanche diodes which could arise from transverse inhomogeneities and thermal effects. All earlier analyses of avalanche-diode microwave oscillators, both small signal and large signal, have been one-dimensional, i.e., the diode is assumed to be homogeneous and uniform in the transverse plane, with infinite transverse dimensions.

---

3. Ruch, J. G. and Kino, G. S., "Measurement of the Velocity-Field Characteristics of Gallium Arsenide," Appl. Phys. Letters, vol. 10, No. 2, pp. 40-42; January, 1967.

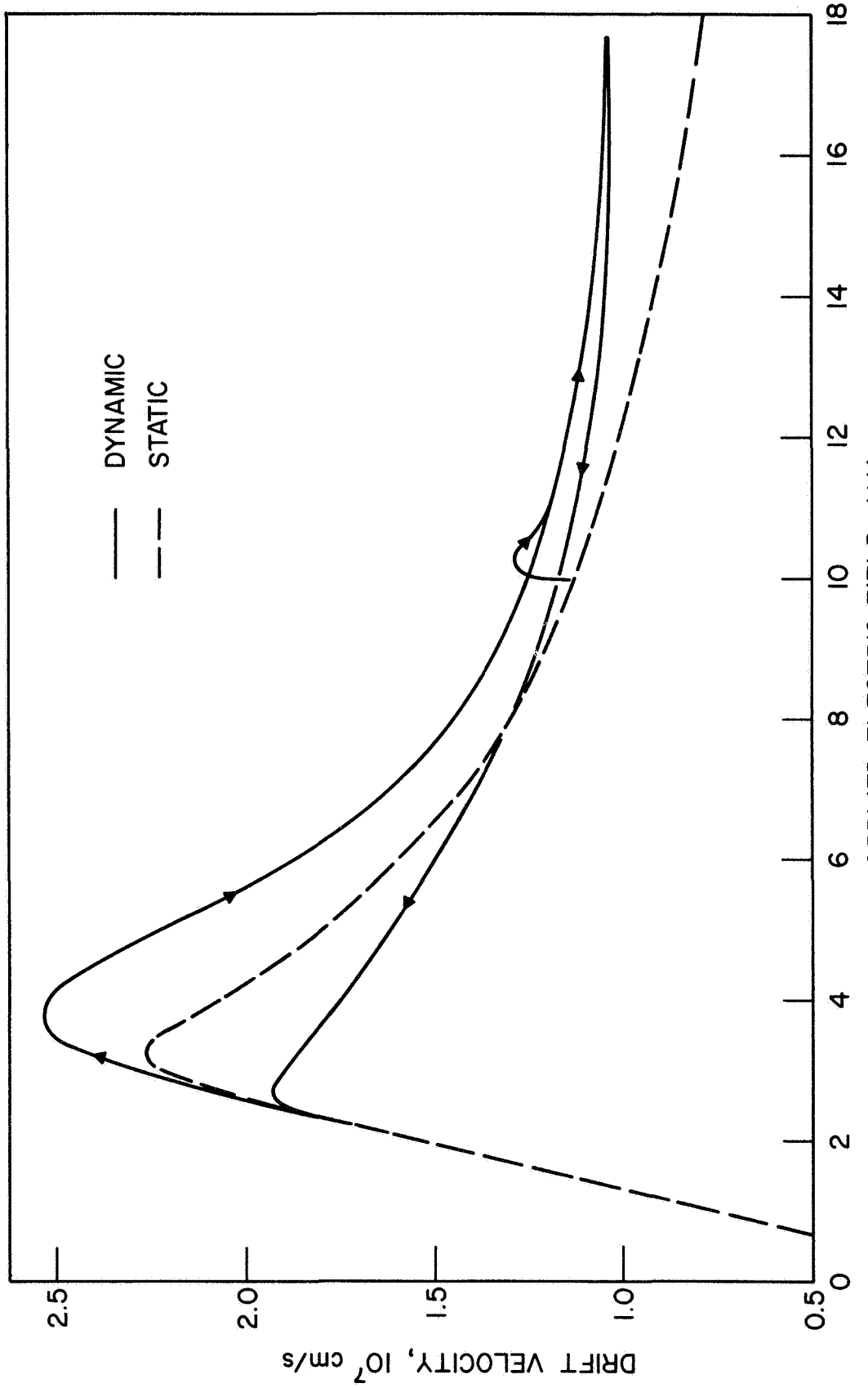

FIG. 6.1 DRIFT VELOCITY AS A FUNCTION OF ELECTRIC FIELD FOR STATIC AND DYNAMIC CASES. (dc BIAS FIELD IS 10 kV/cm, RF FIELD IS 7.7 kV/cm AT 7 GHz)

However, current filaments are known to form in avalanche diodes, and the high-power, large area diodes have considerable transverse nonuniformity. The present analysis will therefore treat a more realistic model of the diode. Some of the advantages of such an investigation are given below.

7.2 Objectives. A two-dimensional analysis of avalanche diodes appears necessary for the following purposes:

1. To determine the effect of different diode geometries and inhomogeneities on diode performance. This would be of importance in the design of avalanche diodes as a part of integrated circuits also.

2. To take into account the effect of the formation of current filaments in the diode, which have been shown to exist both theoretically[1] and experimentally.[2]

3. To understand the frequency sweeping effects and pulse-to-CW transition in avalanche diodes observed recently.[3]

4. To examine the ARP mode theory[4] of high-efficiency oscillations in avalanche diodes. A device with current controlled negative resistance has been shown to be unstable, leading to the formation of a filament.[1] While the ARP mode theory admits the existence of differential negative

---

1. Ridley, B. K., "Specific Negative Resistance in Solids," Proc. Phys. Soc., vol. 82, No. 6, pp. 954-966; 1 December 1963.

2. Barnett, A. M. and Milnes, A. G., "Filamentary Injection in Semi-Insulating Silicon," Jour. Appl. Phys., vol. 37, No. 11, pp. 4215-4223; October, 1966.

3. Buntschuh, C. and Gilden, M., "Integrated Solid State Ku-Band Source," Interim Tech. Report No. 2, Microwave Associates, Inc., Burlington, Mass.; November, 1968.

4. Snapp, C. P. et al., "Experimental Analysis of High-Efficiency Avalanche-Resonance Pumped Oscillators," Electronics Letters, vol. 4, No. 26, pp. 595-596; 27 December 1968.

resistance, it is one-dimensional. It is therefore significant to carry out a two-dimensional analysis to verify the theory.

5. To explain some experimental results recently obtained by Snapp and Hoefflinger[5] on high-efficiency mode of oscillations of avalanche diodes.

7.3 Discussion of Work Performed. During this period, the state of the art of avalanche diodes was surveyed. Some of the best results obtained so far are shown in Fig. 7.1. The relevant literature dealing with the analysis of avalanche diodes and with the study of nonuniformities in semiconductor devices was reviewed and a bibliography was prepared. It was found that very little work has been done on two-dimensional analysis of semiconductor devices in general.

The first step in the two-dimensional analysis of avalanche diodes is a self-consistent and fairly true formulation of equations describing the generation and transport of carriers in the semiconductor material and the associated effects. During this period, efforts were directed towards determining a suitable set of approximations and, based on these, writing a complete set of equations. Very few assumptions were made to keep the formulation of the problem as general as possible. However, further restrictions will be made as necessary to simplify the work involved in the solution. As several changes are anticipated during the process of choosing assumptions in an optimum manner so as to facilitate solution with minimum limitation of applicability, the details of the formulation are not being reported at this time.

---

5. Snapp, C. P. and Hoefflinger, B., "Effect of Space Charge on Efficiency of Avalanche Diodes in Advanced Concepts of Microwave Generation and Control in Solids," Tech. Report No. RADC-TR-68-329, Cornell University, Ithaca, N. Y.; October, 1968.

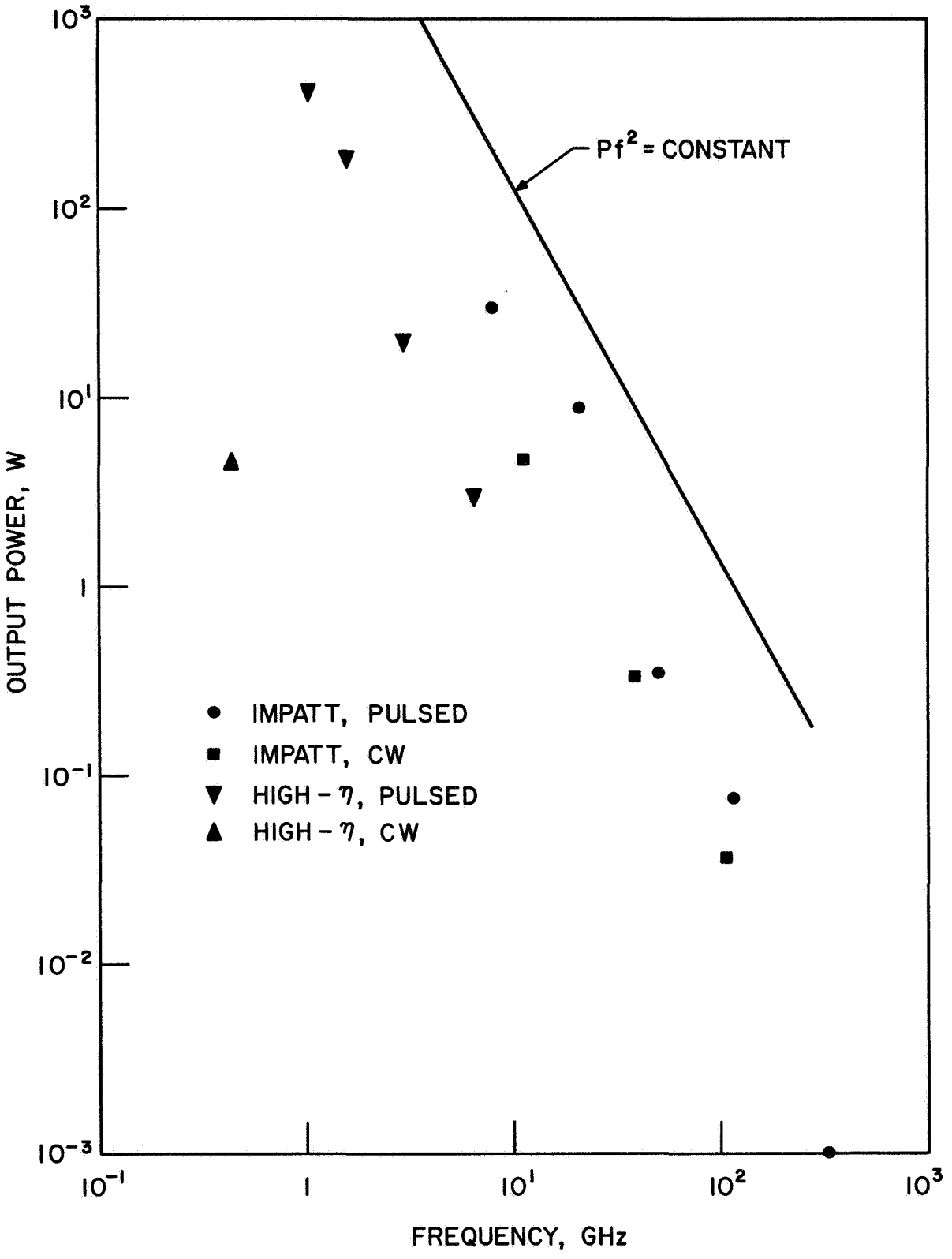

FIG. 7.1 POWER LEVELS AS A FUNCTION OF FREQUENCY ACHIEVED IN AVALANCHE-DIODE OSCILLATORS.

Briefly, the first model of an avalanche diode, cylindrical in shape, contains a current filament of adjustable diameter at the axis due to a large multiplication occurring at the center of a thin avalanche region. The filament suffers diffusion and pinch, and causes nonuniform heating of the semiconductor, resulting in a change in conductivity, and consequent redistribution of current. Steady-state equations for the model are written, taking into account the effect of space charge due to carriers. At present, several effects such as temperature dependence of the multiplication factor and drift velocity, transverse drift of carriers due to space-charge fields, and others, are included in the formulation. Suitable boundary conditions for charge density and temperature are also chosen. Further additions and modifications in the model are currently under consideration.

7.4 Program for the Next Period. It is planned to continue this investigation through the next period with the following objectives. The model of the avalanche diode will be modified, as the need arises, both to increase its accuracy and to make a solution tractable. Effects of a time-dependent flow of carriers, instead of the steady state assumed in the above model, will be evaluated. Attempts will be made at a solution, both analytically and numerically. Pertinent experimental measurements are also under consideration on diodes that will be designed and fabricated in facilities presently under construction in this laboratory.

EPL Memo No. 69-2-08400
17 January 1969
By: G. T. Konrad

ION IMPLANTATION IN SEMICONDUCTORS

I. INTRODUCTION

If a material is bombarded with a beam of ions, some of the ions are retained in the material, some are reflected and some of the substrate material may be sputtered. The physical processes that are involved in the penetration of the host material by the ions appear to be fairly well understood if the substrate is an amorphous substance. The theory developed by Lindhard et al.[1] represents a refinement of various earlier ideas starting with Bohr. This theory, which is based on a Thomas-Fermi potential for the scattering process, assumes the target atoms to be randomly arranged in space. A typical experimental penetration profile consists of a nearly Gaussian peak centered around a most probable penetration distance, R_p, and a long tail representing a deeply penetrating component of relatively low concentration.

For certain orientations of the substrate it was found however that ions can penetrate to anomalously large depths. This is explained as a crystal lattice effect. Certain crystal directions, such as <110> in diamond, present relatively open channels through which an incoming ion may travel. An exact theoretical analysis taking channeling into account has not been made to date because thermal fluctuations of the target atoms and crystalline imperfections (including the surface

preparation of the crystal) prove to be effective dechanneling agents. Completely definitive experimental studies are not possible either because of the difficulty of aligning the ion beam perfectly with the channels in the crystal. Lindhard[2] worked out a theoretical analysis in which he divided the incident ion beam into a random beam and a channeled beam. These beams were treated separately and the final distribution of the implanted ions was obtained by superposition. A review of many of the theoretical considerations involved in these analyses is given by Gibbons.[3]

II. TYPES OF DOPING OBTAINABLE BY ION IMPLANTATION

There are basically three kinds of doping that may be obtained by ion bombardment depending upon the method of implantation and the type of ions used.

1. Bombardment damage doping results when ions such as He^+ are used for bombardment. No ordinary chemical doping effects would be expected in that case but the Fermi level is known to be affected, being moved, for example, toward the center of the band gap in silicon. In this respect bombardment damage produces a doping effect just as conventional chemical dopants do. This was employed in the earliest experiments on ion implantation.

2. Substitutional doping takes place when column III and V element ions are used to bombard silicon and germanium, for example. Proper annealing at the end of the bombardment is usually required to reduce bombardment damage. In addition, it is usually necessary to anneal the target during bombardment so that the ions being presently implanted are

not adversely affected by the atoms deposited in interstitial locations previously.[4,5]

3. Interstitial doping can be obtained when alkali ions are introduced in silicon. Apparently the supersaturation possible is very large. The alkalis form n-type impurities in silicon. Targets of p-type silicon are used for bombardment. A p-n junction is formed at that depth in the substrate where the implanted profile equals the background concentration.

III. EVENTS ACCOMPANYING ION IMPLANTATION

During ion bombardment and for some time thereafter certain physical or chemical processes may take place in the target after the incident ions have given up their kinetic energy and become lodged inside the target.

1. Interstitial-substitutional reactions may occur in which an ion lodged in an interstice of the target crystal moves to a vacancy created by the bombardment or to one that existed before bombardment. Thus fairly extensive post-bombardment annealing is needed not only to move the ions to substitutional sites, but also to remove bombardment damage.[4,7-9]

2. Diffusion of interstitials is frequently quite high in crystals even without bombardment. Thus certain ions may be expected to give rise to diffusion tails even at moderate temperatures. These diffusion tails should follow Fick's law, with the ordinary diffusion coefficient applicable.

3. Drift of the diffusing dopant atoms may take place when an intense electric field is present.

4. Evaporation of the dopant may take place during bombardment because the dopant solubility reaction at the target surface is driven in the forward direction by keV energies, which are magnitudes greater than the thermal energy. Thus an enormous supersaturation of dopant can be produced within the target, which may be relieved by evaporation of dopant from the target surface.

5. Precipitation is another process by which the supersaturated system may try to return to equilibrium.

6. Ion pairing is possible in the case of interstitial dopants, like alkali ions pairing with substitutional acceptor ions.

The above list of processes is an example of the areas of interest in the field of solid-state chemistry. Review articles by McCaldin[10,11] treat these and related aspects in much greater detail.

IV. MEASUREMENT OF JUNCTION DEPTH

One of the major applications of ion implantation appears to be in the production of p-n junctions. As an example of the types of measurements that need to be made after a semiconductor sample has been implanted with ions, a short summary of junction depth determination will be given. Methods have been developed in the past for measuring the depth of a junction by lapping or etching away[3,12] layers of the semiconductor and measuring the surface characteristics at each step. Conductivity or capacitance measurements can be made to find the concentration profile in this way. Implantation can be made with

radioactive tracers, in which case the density profile can also be measured in a stepwise lapping or etching process. A p-n junction location technique is described by Kleinfelder et al.[13] Samples of varying background resistivities are simultaneously made to insure identical implants. The conductivity of the samples is chosen to be opposite to that caused by the ions to be implanted. Thus after implant, every sample contains a p-n junction located at that depth at which the implanted (substitutional) profile concentration exactly equals the background concentration. The junction depth can be measured by a variation of the lapping and staining technique. Thus each sample gives one point on the implanted doping distribution curve. Detection of the implanted concentration over eight orders of magnitude in density below the peak density is possible.

V. APPLICATIONS OF ION IMPLANTATION

Applications for ion implantation in solid-state electronics are immediately apparent from the above discussion.

1. Since the ion beam can be closely controlled, unique doping patterns can be formed which are not possible by other means such as diffusion. Thus intricate semiconductor shapes, such as are required in integrated circuit technology, could be produced.

2. By programming the position or orientation of the substrate during the bombardment time, the density of the dopant as a function of depth in the substrate can be controlled in a prescribed manner. Thus certain graded junctions which would be difficult to achieve otherwise could be produced.

3. Avalanche diodes require very abrupt junctions in order to operate in the millimeter-wavelength region. To date this has limited the capability of diode manufacturers in producing avalanche diodes for the millimeter-wavelength region. Ion implantation promises to be a method for producing very abrupt junctions at a precisely prescribed depth.

4. Lower temperatures (in the range of 400°C to 600°C) can be used in ion implantation doping than in diffusion doping. This minimizes degradation of the host crystal due to pickup of unwanted impurities. This also permits additional design freedom where a number of processing steps must be performed in sequence, as in integrated circuit preparation.

5. Much greater concentrations of dopant can be produced by ion injection than by other methods due to supersaturation. Thus the Fermi level may be pushed to energies not otherwise accessible. Thermoelectric and photovoltaic devices require heavily doped semiconductors for efficient operation. It is believed that the quantum efficiency of certain photocathodes can be enhanced by using heavily doped semiconductors. Furthermore, tunnel diodes require heavy doping and abrupt junctions for successful operation. Thus ion implantation is potentially useful in the improvement of all these classes of devices.

6. Doped surface regions may permit electrical contacts to be made that are otherwise difficult to achieve. In some materials, bombardment produces a surface layer of radically different structure overlying the host crystal which affords useful electrical contact to the latter.

VI. PROPOSED EXPERIMENTAL FACILITY

It is suggested that as much as possible of the present relativistic beam experimental facility be adapted for the ion implantation device. In particular, some of the power supplies, the vacuum chamber and the vacuum pumps should be useful. Figure 1 shows a diagram of the overall ion beam handling facility. A gun, which will be described more fully below, produces a 10 kV ion beam of the particular species desired for implantation. A lens system is used for focusing the beam. Since there are likely to be some impurities of different mass number in the ion beam it is desirable to incorporate a mass separator. It is proposed to use purely electric means for mass separation[14] because a magnetic mass separator is quite bulky. The deflection plates are for final adjustment of the position of the ion beam. If a sawtooth voltage is applied, then the beam can be swept over the target area in order to obtain a greater implantation uniformity.

6.1 Quadrupole Mass Analyzer

Use is made of the time-dependent acceleration of an ion in a high-frequency electric field applied to an electric quadrupole. The distribution of the electric field in space is characterized by a purely quadratic function of the coordinates. If ions are introduced into such a field, their equations of motion lead to differential equations with periodic coefficients. These equations are characterized by stable and unstable solutions. If e/M of an ion corresponds to a stable region, then all possible trajectories are stable and if e/M corresponds to an unstable region in the solution, then all possible trajectories are

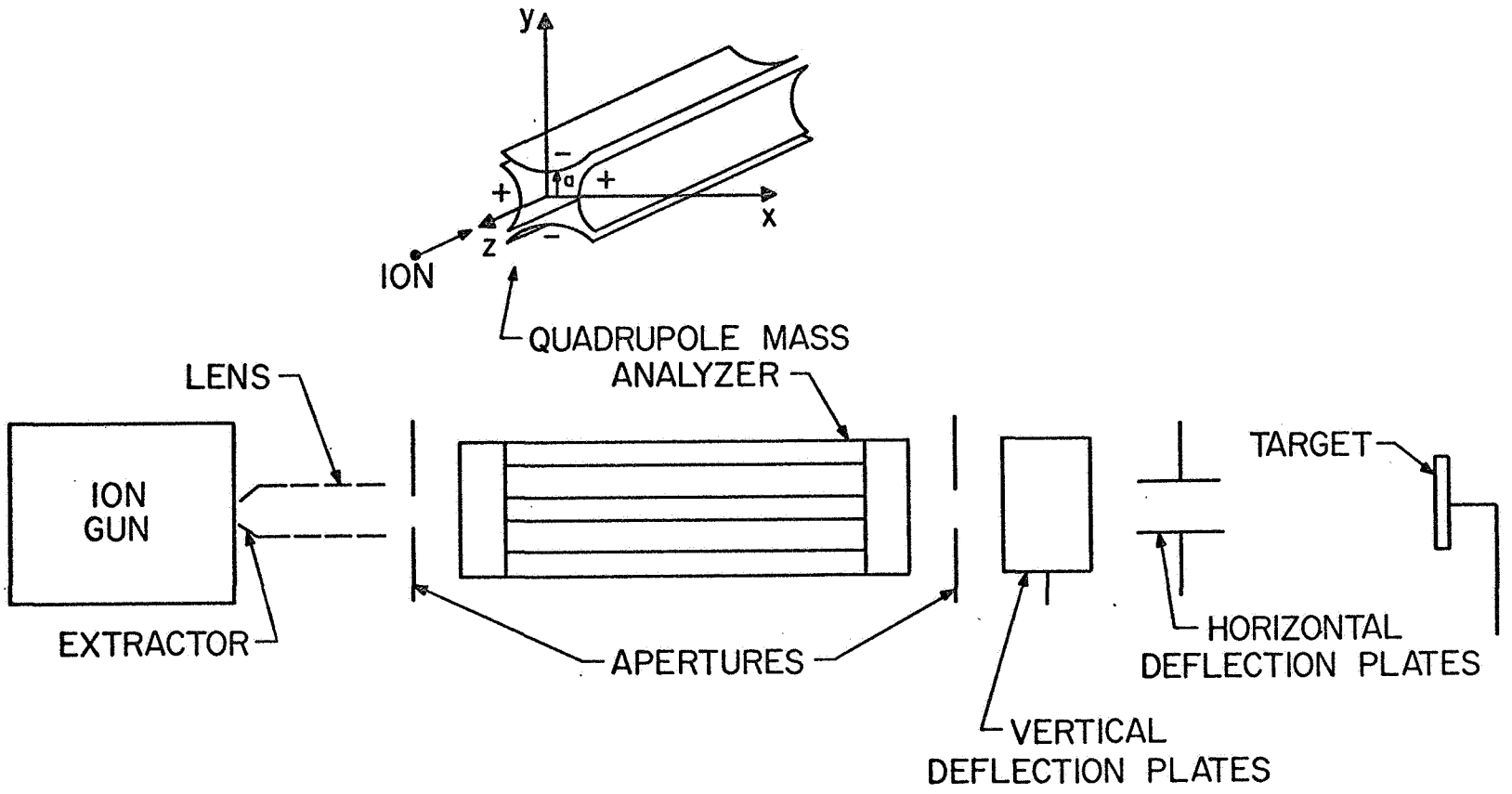

FIG. 1 ION BEAM SYSTEM.

unstable. This situation can be realized by a symmetric quadrupole field existing between a set of hyperbolic electrodes as shown in Fig. 1. A voltage $1/2(U + V \cos \omega t)$ is applied to the electrodes marked + and a voltage $-1/2(U + V \cos \omega t)$ is applied to the electrodes marked -. Here U is a dc voltage component. The potential at any point (x,y) is then given by

$$\varphi(x,y,t) = \left(\frac{U + V \cos \omega t}{a^2}\right)\left(\frac{x^2 - y^2}{2}\right)$$

and the equations of motion for an ion are

$$\ddot{z} = 0 ,$$

$$\ddot{x} - \frac{2e}{Ma^2}(U + V \cos \omega t)\cdot x = 0$$

and

$$\ddot{y} + \frac{2e}{Ma^2}(U + V \cos \omega t)\cdot y = 0 .$$

This leads to Mathieu's equation

$$\frac{d^2x}{d\zeta^2} + (\lambda + q \cos 2\zeta)x = 0 ,$$

where

$$2\zeta = \omega t ,$$

$$\lambda = \frac{4eU}{Ma^2\omega^2}$$

and

$$q = \frac{4eV}{Ma^2\omega^2} .$$

There are only certain regions for the parameters λ and q for which a stable solution, i.e., a solution which is finite for all initial values of ωt, can be obtained. Outside of these stable regions the solutions grow exponentially and the ions involved are intercepted on the electrodes. Thus, this arrangement of electrodes acts as a mass analyzer which lets ions in a mass region M_1 to M_2 pass through but draws all other ions to the electrodes. Experimentally, the electrodes may be approximated by four cylindrical rods to which the proper voltage $U + V \cos \omega t$ is applied. As an example, for a = 1 cm, V = 1500 V, U = 256 V and $M = 1.6 \cdot 10^{-25}$ kg (100 AMU) it turns out that $\omega/2\pi = 1$ MHz.

6.2 Ion Source

It is proposed to use an ion source that can produce ions from gaseous as well as solid substances.[15] Such a source is shown in Fig. 2. There are two filaments needed in the gun. One is for heating the anode and the crucible containing the solid substance from which ions are to be obtained. The other is for furnishing electrons. The electrons spiral inside the anode chamber due to the presence of the magnetic field. This ionizes the gas particles and forms a plasma. The positive ions are withdrawn by the extractor electrode through the anode hole. An extraction voltage of approximately 10 kV can be used.

6.3 Collector

The collector shown in Fig. 3 is intended to be operated at a high negative potential so that the ions can be given their final acceleration up to 100 kV. A sample holder is mounted inside the ion collector. The target can be moved from outside the vacuum chamber. A resistive heater

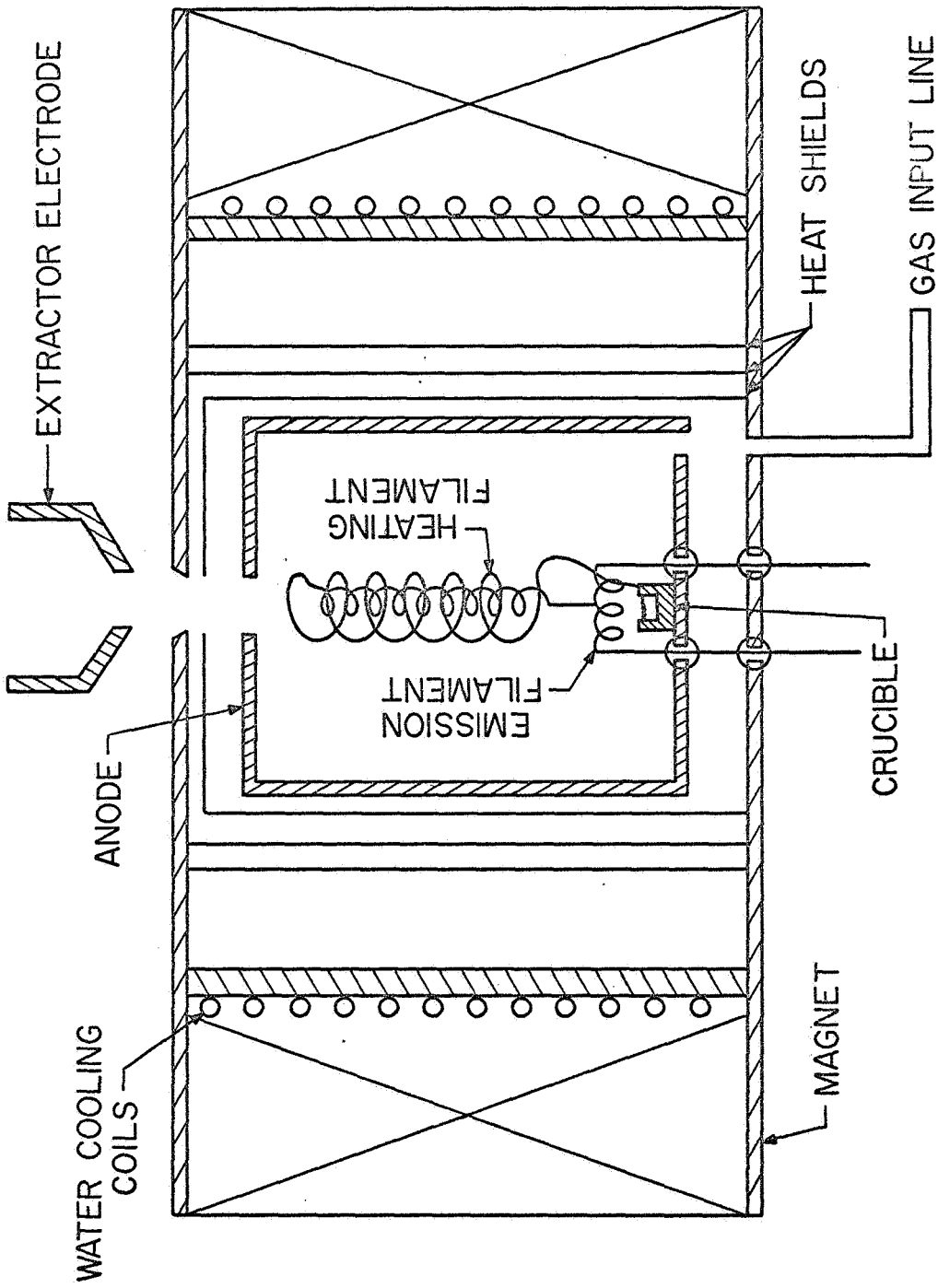

FIG. 2 METAL ION SOURCE.

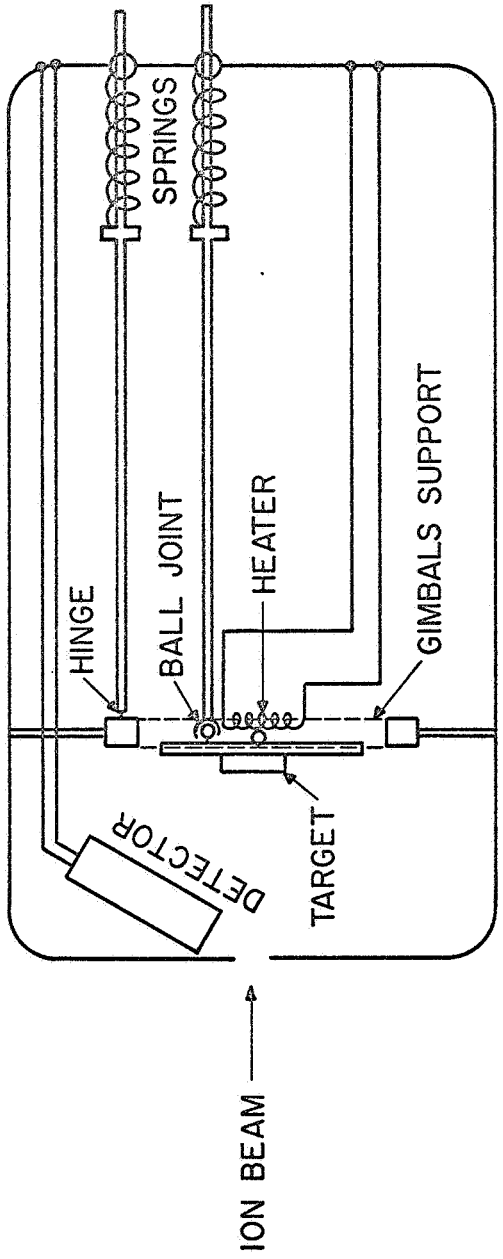

FIG. 3 COLLECTOR AND TARGET.

is mounted near the sample holder so that implantation can proceed at the proper temperature and the sample can be annealed after implantation. A thermocouple is present for monitoring the temperature. Before the sample can be implanted it must be oriented properly. This can be done by bombarding the target with a beam of protons and monitoring the reflected protons with a NaI detector while the sample is positioned until the crystal axes are properly aligned with the ion beam.

6.4 Overall System

The vacuum system and chamber proposed to be used are shown in Fig. 4. There are two viewing ports, one near the gun end and one on top of the chamber. The collector and its high voltage connections are mounted from the big flange which has been the collector flange in the REB experiment. Two vacuum pumps with appropriate valves are used as shown. A diffusion pump is included for rough pumping the chamber and maintaining a good vacuum in the ion gun. The ion pump may be opened to the system when a pressure in the 10^{-5} Torr range has been obtained. A ball valve should be installed in the channel just outside the ion gun so that the gun or the system can be opened to air without affecting the vacuum in the other. It is expected that the gun will have to be opened to air frequently in order to change filaments and the implanting material. Thus the gun should be readily demountable.

VII. PROPOSED INITIAL WORK

First the apparatus described above needs to be built. Outside vendors are available to do part of this. Two sources would be High

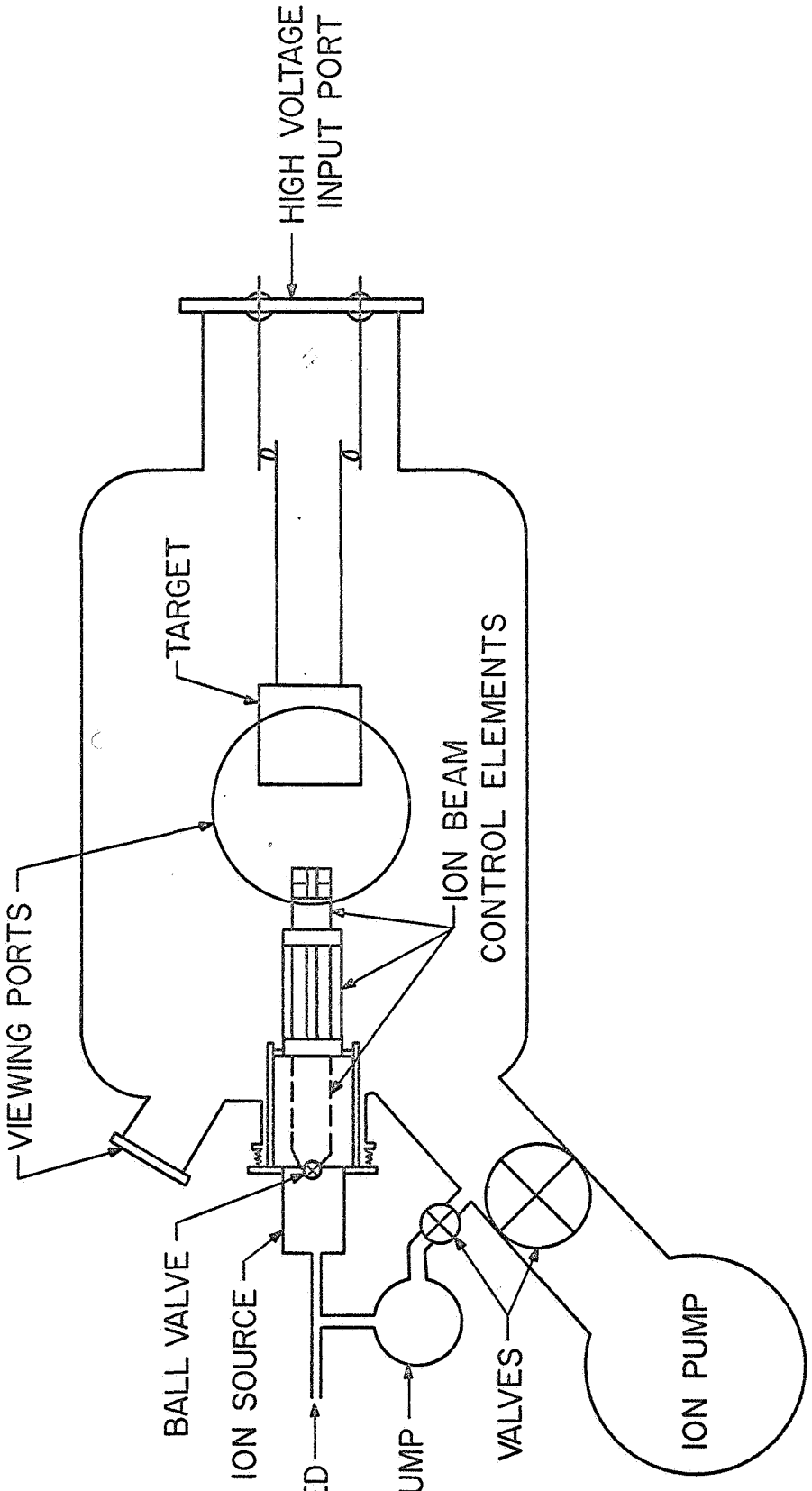

FIG. 4 ION IMPLANTATION EXPERIMENTAL LAYOUT.

Voltage Engineering Corporation and Varian Associates. The former may have some of the parts for the ion source, while the latter could furnish some of the vacuum components.

A semiclean room should be set up on North Campus to store and prepare the samples for implantation. The darkroom we presently occupy there should be ideally suited since hot and cold water as well as sinks are readily available and since it is outside the heavily used portion of the work areas.

After the samples have been implanted it is necessary to be able to do the following.

1. Process doped materials to desired characteristics (annealing, multiple doping, preparing samples for specific uses).

2. Evaluate doped materials (distribution of doping profile, characteristics of p-n junctions formed, etc.).

3. Apply appropriate thin layers to certain substrates for implantation and apply electrical contacts after implantation (an evaporator would be needed for this).

It would be desirable to do as much of this as possible on North Campus close to the implantation facility in order to conserve time but most importantly to reduce chances for contamination.

LIST OF REFERENCES

1. Lindhard, J. et al., "Range Concepts and Heavy Ion Ranges," Mat. Fys. Medd. Dan. Vid. Selsk., vol. 33, No. 14, pp. 1-42; 1963.

2. Lindhard, J., "Influence of Crystal Lattice on Motion of Energetic Charged Particles," Mat. Fys. Medd. Dan. Vid. Selsk., vol. 34, No. 14, pp. 1-64; 1965.

3. Gibbons, J. F., "Ion Implantation in Semiconductors-Part I. Range Distribution Theory and Experiments," Proc. IEEE, vol. 56, No. 3, pp. 295-319; March, 1968.

4. Gibbons, J. F. et al., "Implantation Profiles for 40-keV Phosphorus Ions in Silicon Single-Crystal Substrates," Appl. Phys. Letters, vol. 8, No. 2, pp. 46-48; 15 January 1966.

5. Glotin, P. M., "Influence of Temperature on Phosphorus Ion Behavior During Silicon Bombardment," Canadian Jour. Physics, vol. 46, No. 6, pp. 705-712; 15 March 1968.

6. Medved, D. B. et al., "Implantation and Channeling Effects of Alkali Ion Beams in Semiconductors," Nucl. Instr. and Methods, vol. 38, No. 3, pp. 175-177; December, 1965.

7. Alton, G. D. and Love, L. O., "Radiation Damage and Substitutional Chemical Impurity Effects in Single-Crystal Germanium Bombarded with 40-keV B^+, Al^+, Ga^+, Ge^+, P^+, As^+, and Sb^+ Ions," Canadian Jour. Phys., vol. 46, No. 6, pp. 695-704; 15 March 1968.

8. Martin, F. W. et al., "Junction Counters Produced by Ion Implantation Doping," IEEE Trans. on Nuclear Science, vol. NS-11, No. 3, pp. 280-285; June, 1964.

9. Dearnaley, G. et al., "Implantation Profiles of ^{32}P Channeled into Silicon Crystals," Canadian Jour. Phys., vol. 46, No. 6, pp. 587-595; March 15, 1968.

10. McCaldin, J. O., "The Doping of Semiconductors by the Injection of Energetic Ions," Progress in Solid State Chemistry, vol. 2, H. Reiss (Ed.), Pergamon Press, Ltd., London, Chap. 2, pp. 9-25; 1965.

11. McCaldin, J. O.,"Ion Beams and Solid State Physics," Nucl. Instr. and Methods, vol. 38, No. 3, pp. 153-164; December, 1965.

12. Tannenbaum, E., "Detailed Analysis of Thin Phosphorus Diffused Layers in p-Type Silicon," Solid-State Electronics, vol. 2, No. 2/3, pp. 123-132; March, 1961.

13. Kleinfelder, W. J. et al., "Impurity Distribution Profiles in Ion-Implanted Silicon," Canadian Jour. Phys., vol. 46, No. 6, pp. 597-606; 15 March 1968.

14. Paul. W. and Raether, M., "Das Elektrische Massenfilter," Z. Physik, vol. 140, No. 3, pp. 262-273; 1955.

15. Magnuson, G. D. et al., "High Efficiency Source for Metal Ions," Rev. Sci. Instr., vol. 36, No. 2, pp. 136-142; February, 1965.